Picosecond Time-Resolved Coherent Anti-Stokes Raman Spectroscopy of the Artificial Bacteriorhodopsin Pigment, BR6.11†

Andrew C. Terentis, Yidong Zhou, and George H. Atkinson*

Department of Chemistry and Optical Sciences Center, University of Arizona, Tucson, Arizona 85721

Laszlo Ujj

Department of Physics, University of West Florida, Pensacola, Florida 32514

Received: May 13, 2003; In Final Form: July 24, 2003

The picosecond molecular dynamics in an artificial bacteriorhodopsin (BR) pigment, BR6.11, are measured by picosecond time-resolved coherent anti-Stokes Raman spectroscopy (PTR/CARS) and picosecond transient absorption (PTA). The BR6.11 pigment contains a structurally modified retinal chromophore with a six-membered carbon ring bridging the C_{11}═C_{12}−C_{13} bonds, which both locks the C_{11}═C_{12} bond in the trans configuration and prevents rotation about the C_{12}−C_{13} bond. The changes in the vibrational degrees of freedom of the retinal attributable to the six-membered carbon ring are found in the picosecond resonance CARS (PR/CARS) spectrum of ground-state BR6.11. Normal mode assignments for more than forty BR6.11 vibrational features are made through comparisons with the PR/CARS data from native BR-570 (previously analyzed in terms of the selective isotopic substitution of the retinal). PTR/CARS spectra from two intermediates (J6.11 and K6.11), observed by PTA to appear during the initial 200 ps of the BR6.11 photocycle, reveal distinct retinal structures for each. The retinal in J6.11 contains delocalized (i.e., vibrational degrees of freedom not well described by normal modes and spanning major regions of the retinal), out-of-plane motion, and a highly twisted all-trans polyene configuration while K6.11 contains a retinal in which vibrational degrees of freedom have relaxed into well-defined, out-of-plane normal modes and a less twisted (though markedly nonplanar), 13-cis configuration. These vibrational data show that C_{13}═C_{14} isomerization is not the first structural change to occur in the BR6.11 photocycle, but rather is the principal structural change during the J6.11 to K6.11 transformation. The similarity of the retinal structural dynamics in the BR6.11 and native BR-570 photocycles demonstrates that subpicosecond, torsional motion within the polyene precedes C_{13}═C_{14} isomerization and is critical for initiating the BR photoreactivity underlying their biochemical function. The structural dynamics comprising the initial 200 ps of the BR6.11 photocycle, as derived from these PTR/CARS data, are described well by a three-state model in which J6.11 and K6.11 are assigned as excited and ground electronic states, respectively.

Introduction

The purple membrane of the archaebacterium, *Halobacterium salinarum*, contains a single trans-membrane protein, bacteriorhodopsin (BR), that stores and utilizes absorbed light energy to transport protons across the cell membrane.[1−3] The resulting potential gradient created across the cell membrane drives ATP synthesis.[3] The high efficiency of the BR molecular mechanism, as well as its role as a prototype for other, more complicated ion transporting proteins, underlies much of the biochemical interest in BR.

Although many features of the energy storage mechanism within BR are reasonably well characterized,[4,5] the dynamics of the initial structural changes in the retinal chromophore are still to be fully understood. Of particular interest are those structural changes occurring during the initial femto/picosecond period of the BR photocycle. Trans to cis isomerization of the C_{13}═C_{14} bond has been widely viewed in earlier models of the BR photocycle as the primary molecular event.[1,6] These models also assume that all-trans to 13-cis isomerization within retinal occurs prior to the 0.5 ps appearance of the J-625 intermediate.[1,6] Recently,[7] however, picosecond time-resolved coherent anti-Stokes Raman spectra (PTR/CARS) indicate that J-625 contains an all-*trans*-like retinal. Specifically, the C−C stretching band ("fingerprint") pattern, used widely in vibratonal spectroscopy to identify the retinal configuration,[1] remains almost unchanged as J-625 is formed from BR-570 (all-trans), but changes significantly as K-590 (13-cis) subsequently (3.5 ps) appears.[7] Thus, J-625 is an intermediate in which the retinal structure has undergone significant changes relative to BR-570 (vide infra), but C_{13}═C_{14} isomerization is not one of them. The change from all-trans to 13-cis retinal occurs during the J-625 to K-590 transformation.

The structural properties of the J-625 retinal that distinguish it from those in BR-570 and K-590 include the following: (i) increased electron density in the C═C bonds (increased C═C stretching mode frequencies), (ii) significant "delocalized" hydrogen out-of-plane (HOOP) motion, and (iii) a Schiff-base bonding environment similar to that of BR-570, but distinctively different from that in K-590. These vibrational CARS features indicate that J-625 has a highly distorted (twisted) retinal

* To whom correspondence should be addressed. E-mail: atkinsog@u.arizona.edu.

† Part of the special issue "Charles S. Parmenter Festschrift".

10.1021/jp030612g CCC: $25.00
Published on Web 09/20/2003

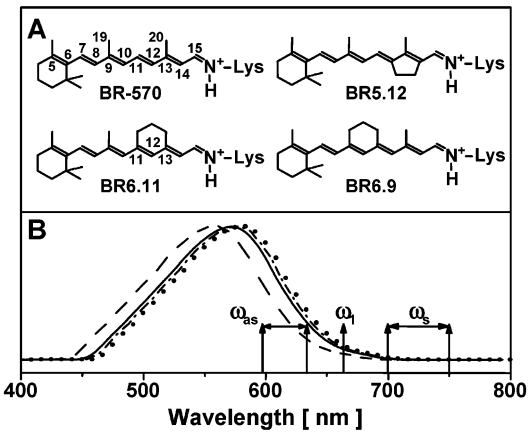

Figure 1. (A) Chemical structures of retinal chromophores in BR-570, BR5.12, BR6.9, and BR6.11 and (B) absorption spectra of BR-570 (solid line, intensity maximum at 568 nm), BR5.12 (dotted line, intensity maximum at 578 nm), BR6.9 (dot−dash line, intensity maximum at 572 nm), and BR6.11 (dashed line, intensity maximum at 556 nm). The pump ($\omega_1 = 663$ nm) and probe ($\omega_s = 700-750$ nm) wavelengths used to obtain PR/CARS spectra from BR6.11 are shown at the bottom together with the spectral region (595−635 nm) where the ω_{as} signal appears.

conformation, an observation that is consistent with earlier time-resolved resonance Raman results.[8] The third type of difference also supports the idea that trans to cis retinal isomerization does not occur until K-590 is formed, whereby the retinal Schiff base proton moves to a different position within the protein pocket.

"Delocalized" out-of-plane retinal motion connotes vibrational energy not well described by normal modes. Appearing as highly broadened (>50 cm^{-1}) vibrational features, delocalized out-of-plane motion is distributed over major regions of the retinal, and therefore differs from out-of-plane motion observed as unbroadened (<5 cm^{-1}) bands that are well represented by the normal mode approximation. The appearance and time-dependent evolution of these two types of out-of-plane vibrational motion is a distinguishing characteristic of J-like intermediates.

The PTR/CARS spectrum of K-590 also contains strong bands corresponding to HOOP and out-of-plane methyl vibrational modes, although these bands are neither as intense or broad as those in the spectrum of J-625.[7] Overall, the K-590 PTR/CARS data are consistent with both X-ray crystallographic data[9−11] and molecular dynamics simulations[12,13] showing the retinal in K-590 to have a 13-cis configuration but with a strongly deformed, out-of-plane structure. Simulations suggest that strong torsions appearing mainly in the $C_{12} \sim N$ region of the K-590 retinal[12] are associated with weakening[12] or breaking[11] of H-bonding between the Schiff base of the chromophore and a neighboring water molecule (w402) occupying a bridging position within the protein binding pocket. This disruption of the H-bonding network is proposed as a mechanism for the temporary storage of absorbed photon energy in the K-590 intermediate.[12]

The work presented here seeks to more clearly characterize the structural changes in the retinal that define the primary reaction coordinates within the BR photocycle. The relationship of these changes in retinal structure to C_{13}═C_{14} isomerization is of special interest. Since out-of-plane retinal motion has been shown in BR to be important,[7,8,11−13] attention is focused on examining the femto/picosecond structural events in a series of structurally related artificial BR pigments containing aliphatic carbon rings that selectively isolate motion around specific C−C and C═C bonds (Figure 1). By the selective limitation of out-of-plane motions and/or C═C isomerization throughout the retinal, the contributions of these two types of retinal structural changes can be determined. The six-membered carbon ring in the retinal of BR6.11 examined here blocks the permanent isomerization and/or rotation in the C_{11}═C_{12}−C_{13} region (Figure 1) but does not directly prevent C_{13}═C_{14} isomerization. Thus, a comparison of the dynamics in BR6.11 with those in the native BR-570 examines the importance of torsional motions in the C_{11}═C_{12}−C_{13} bonds with respect to the BR photocycle.

The BR6.11 photocycle observed by PTA measurements[14] contains intermediates analogous to those found in the native BR photocycle, and an independent study shows that BR6.11 has a similar biochemical function.[15] The important difference between BR6.11 and BR-570 appears in the decay rates of the respective J intermediates (i.e., J6.11 → K6.11 is 12 ps[14] and J-625 → K-590 is 3.5 ps[6,16,17]). None of these absorption data, of course, provide direct measurements of the structural properties of BR6.11 or of the intermediates composing its photocycle. The vibrational spectrum from BR6.11 and K6.11 have been recorded using time-resolved RR spectroscopy, but only at relatively low spectral resolution.[18]

Previous PTR/CARS experiments examined the photoreactions of two different artificial BR pigments, BR5.12[19] and BR6.9[20] (Figure 1). Each of these artificial BR pigments selectively restricts motion at specific retinal bonds, and therefore, by viewing the associated dynamics collectively, an understanding of the changes in retinal structure critical to the BR photocycle can be obtained.

The retinal in BR5.12 contains a rigid, five-membered carbon ring spanning the C_{12}−C_{13}═C_{14} bonds that locks the C_{13}═C_{14} bond in the trans configuration. Consequently, BR5.12 displays no proton-pumping activity,[21] and its photoreaction contains only a single, red-shifted photointermediate, T5.12(J5.12), that decays directly back to the ground state with a time constant of 17−19 ps.[22,23] PTR/CARS spectra show the T5.12(J5.12) retinal to have (i) increased out-of-plane (HOOP) motion relative to BR5.12, but without the significant band broadening observed in J-625 and (ii) increased pi-electron density in C═C bonds, but no C_{13}═C_{14} isomerization (as expected for this ring-locked pigment).[19] The overall similarity of the C−C stretching band pattern in T5.12(J5.12) and J-625 supports the conclusion that the retinals in both are all-trans-like and that trans-cis C_{13}═C_{14} isomerization occurs only when the J-like intermediates decay to a K-like intermediate.[7]

The retinal in BR6.9 contains a six-membered carbon ring spanning the C_9═C_{10}−C_{11} bonds (Figure 1). PTA and PTR/CARS data from BR6.9 reveal two distinct intermediates, J6.9 and K6.9, with lifetimes of 5 ps and >50 ns, respectively.[20] Independently, BR6.9 has been shown to have biochemical activity similar to that in BR-570.[15] Other than slowing the formation and decay rates for the intermediates, these data show that restricting retinal motion at the C_9═C_{10}−C_{11} bonds does not significantly alter the photocycle mechanism of BR.

The higher (temporal and spectral) resolution of the PR/CARS and PTR/CARS data from BR6.11 presented here (as compared to previous time-resolved RR data[18]) are used to examine the role of C_{11}═C_{12}−C_{13} bond torsions and C_{13}═C_{14} isomerization. Distinct retinal structures are identified from the spectra of BR6.11, J6.11, and K6.11. Specifically, C_{13}═C_{14} isomerization occurs in the transition from J6.11 to K6.11 while J6.11 is characterized by the same intense, delocalized HOOP motions that are observed in J-625. These experimental CARS results support the conclusions reached from earlier CARS studies that strong, delocalized, out-of-plane vibrations of the polyene chain precede the trans-cis isomerization of the C_{13}═C_{14} bond.

Finally, these CARS results are discussed in terms of a three-state model used to describe the dynamics controlling the initial stages of the BR photoreactivity in both BR6.11 and in BR pigments in general. The consistency between the PTR/CARS data presented here and a three-state model indicates that J6.11, and J species in general, be assigned as excited electronic states, while K6.11, and K species in general, be assigned as ground electronic states.

Materials

The BR samples are grown from a cell line of *Halobacterium salinarum* and are purified according to established methods.[22,24] The purple membrane typically has an absorbance ratio of 1.5 (protein absorbance (280 nm)/retinal absorbance (570 nm)) and is used without further purification. The isolated bacterio-opsin is obtained by removing the all-trans retinal chromophore from BR-570 by a bleaching procedure: BR-570 is bleached for ~48 h by focusing the output of a 500-W projector lamp through a 450-nm cutoff filter onto a light-adapted BR solution containing 1 M NH_3OHCl, 1 M NaOH and 1 M NaCl buffered at pH = 7.0. After bleaching, the sample is centrifuged and washed with 10 mM K_2HPO_4/dithiothreitol (DTT) buffer and 5% v/v solution of bovine serum albumin (BSA) to eliminate the hydroxylamine and any residual all-trans retinal. BR6.11 is prepared by reconstituting the remaining opsin with the structurally modified retinal *E*-11,20-ethanoretinal (Ret6.11). The Ret6.11 is dissolved in ethanol and added to the buffered opsin solution (<2% final volume of ethanol with a 1:1 molar ratio of opsin to retinal). The reconstitution of opsin with Ret6.11 is performed in the dark at 4 °C.

The reconstituted BR6.11 sample is washed and centrifuged with BSA to obtain a pellet that is re-suspended in 10 mM K_2HPO_4/1 mM DTT buffer to yield approximately 15 mL of a 3.5 OD/cm (at 556 nm) sample. All BR6.11 samples are light-adapted by exposure to the output from a fluorescent lamp for approximately 15 min prior to each PTR/CARS measurement. It has been shown that following light adaptation the retinal in BR6.11 adopts an all-trans configuration.[15] PR/CARS and PTR/CARS data measured from the sample on different days following several light adaptation cycles are reproducible, thereby demonstrating that the light adaptation procedure does not cause any significant sample degradation. To avoid any sample degradation during both CARS and PTA experiments, the sample temperature is maintained at ~10 °C, and excitation laser pulse energies are kept to a minimum (<20 nJ/pulse).

Instrumentation and Experimental Procedures

The instrumentation used to record PTR/CARS signals includes three picosecond dye lasers synchronously pumped by the second harmonic output of a cw, mode-locked Nd:YAG laser, an optical system to steer the laser beams, a flowing sample compartment, and a CCD detection system discussed in detail elsewhere.[25,26] Briefly, light pulses from a narrowband (<4 cm^{-1}, fwhm) dye laser operated at 663 nm (ω_1) and a broadband (~700 cm^{-1}) dye laser operated in the 700−750 nm region (ω_s) are phase-matched in a flowing BR6.11 sample, generating CARS signals spanning ~700 cm^{-1} (ω_{as}). These signals are dispersed onto the surface of a liquid nitrogen cooled 2D CCD detector (EG&G 256 × 1024) operated in the focal plane of a triple-stage monochromator (SPEX Triplemate). The CARS signals from BR6.11 solutions are normalized against reference signals from solvent (buffer) alone to isolate the resonant CARS signal from BR6.11.[27] The photoreaction of BR6.11 is initiated via a 570 nm optical excitation beam (ω_{exc}) that is counter-propagated relative to the directions of the ω_1 and ω_s CARS probe beams, thereby avoiding any residual linear and nonlinear scattering signals that would otherwise be observable. All of the dye lasers are operated at a 400 kHz repetition rate to match the flow properties of the liquid sample jet.[25,28] The cross-correlation time (CCT) between the ω_1 and ω_{exc} pulses is 8 ps.

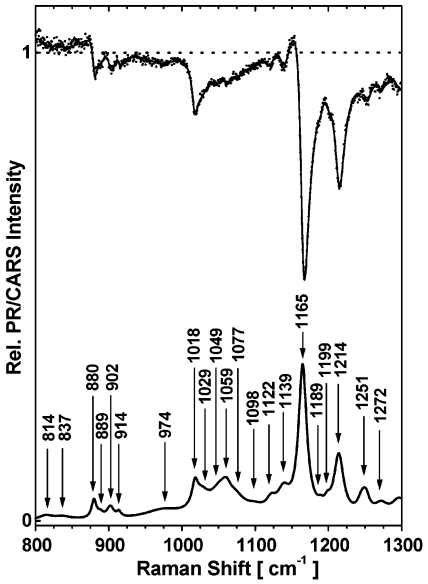

Figure 2. (Top) PR/CARS spectrum of BR6.11 in the 800−1300 cm^{-1} region. The nonresonant CARS signal from water is used to normalize the PR/CARS signal to 1.0 (indicated by the horizontal dashed line). The $\chi^{(3)}$-fit function is shown as a solid line overlapping the PR/CARS data (●). (Bottom) Background-free (Lorentzian line shapes) PR/CARS spectrum of BR6.11 derived from the $\chi^{(3)}$-fit. The wavenumber positions of selected bands are shown as vertical arrows. The $\chi^{(3)}$-fit parameters and a complete list of band origin positions, bandwidths, and relative intensities obtained are presented in Table 1.

PR/CARS and PTR/CARS signals are recorded in alternating order to facilitate the direct comparison of the signals from the ground state BR6.11 and from the reactive mixtures of the transient intermediates. Picosecond transient absorption (PTA) data are recorded during each PTR/CARS experiment to independently measure the relative concentrations of BR6.11 and J6.11 or K6.11 (used in the quantitative $\chi^{(3)}$ analysis of the CARS data) and to accurately determine the 0 ps time point.

The CARS spectra are fitted with a model function described elsewhere.[26] By using the nonlinear fitting procedure, the vibrational parameters (amplitude, bandwidth, vibrational origin, relative electronic phases) describing the vibrational modes of each BR species are determined and a vibrational spectrum containing Lorentzian line shapes is derived.

Results

I. Ground-State BR6.11. *A. PR/CARS Spectrum of BR6.11.* The vibrational spectrum of ground-state BR6.11 reflects the initial chromophoric structure from which its photocycle begins, and therefore, it is the starting point for any vibrational analysis of the retinal structure in photocycle intermediates. The S/N in the RR data (900−1700 cm^{-1} region) for BR6.11[18] limited the observable features to only the six major bands (at 1589 cm^{-1}, 1510 cm^{-1}, 1210 cm^{-1}, 1164 cm^{-1}, 1016 cm^{-1}, and 880 cm^{-1}). In contrast, PR/CARS spectra from BR6.11 (800−1700 cm^{-1} region, Figures 2 and 3) contain more than forty distinct vibrational features. PR/CARS data are recorded from the light-adapted BR6.11 over two spectrally overlapping regions, each spanning 500 cm^{-1}. The 663-nm wavelength of ω_1 is selected

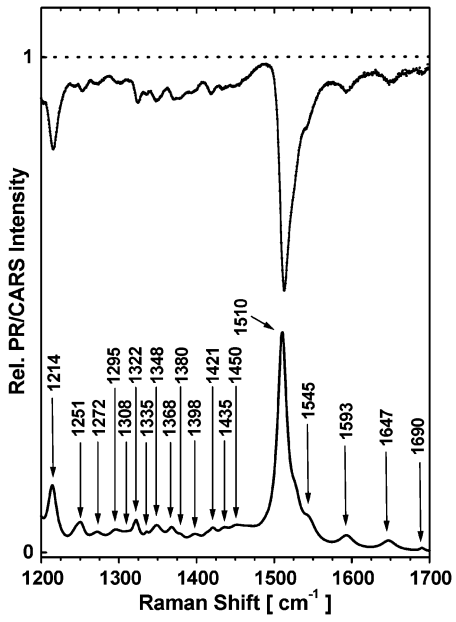

Figure 3. (Top) PR/CARS spectrum of BR6.11 in the 1200−1700 cm^{-1} region. The nonresonant CARS signal from water is used to normalize the PR/CARS signal to 1.0 (indicated by the horizontal dashed line). The $\chi^{(3)}$-fit function is shown as a solid line overlapping the PR/CARS data (●). (Bottom) Background-free (Lorentzian line shapes) PR/CARS spectrum of BR6.11 derived from the $\chi^{(3)}$-fit. The wavenumber positions of selected bands are shown as vertical arrrows. The $\chi^{(3)}$-fit parameters and a complete list of band origin positions, bandwidths, and relative intensities obtained are presented in Table 1.

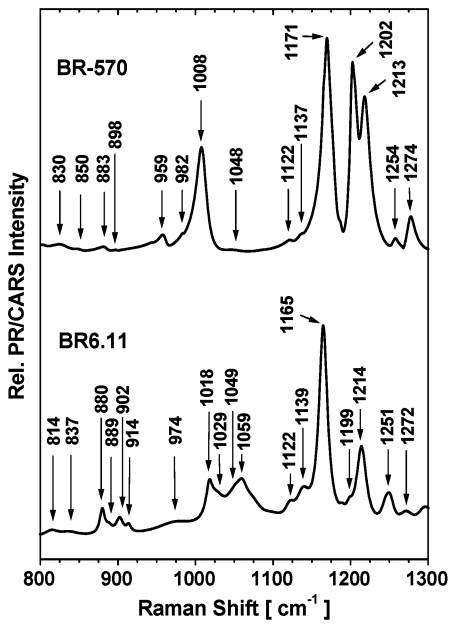

Figure 4. (Top) Background-free (Lorentzian line shapes) PR/CARS spectrum (800−1300 cm^{-1}) of BR-570 and (Bottom) BR6.11. Band positions are origin (Ω_k) values derived from $\chi^{(3)}$ fits of the PR/CARS data (Table 1).

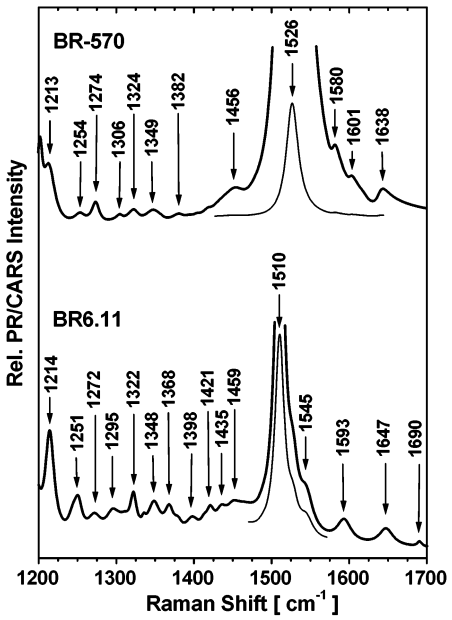

Figure 5. (Top) Background-free (Lorentzian line shapes) PR/CARS spectrum (1200−1700 cm^{-1}) of BR-570 and (Bottom) BR6.11. Band positions are origin (Ω_k) values derived from $\chi^{(3)}$ fits of the PR/CARS data (Table 1).

to occur on the low-energy side of the BR6.11 absorption spectrum (Figure 1) to minimize any contributions to the CARS signal from photocycle intermediates. While the absorption spectrum of BR6.11 is slightly blue-shifted (556 nm peak) relative to BR-570 and other artificial pigments (e.g., BR6.9 at 572 nm[20] and BR5.12 at 578 nm,[19] Figure 1), the excitation conditions employed are sufficiently similar to those used in previous studies of other BR pigments to warrant a direct comparison of the respective PR/CARS spectra, vide infra.

The $\chi^{(3)}$-fitting functions for PR/CARS data of BR6.11 are used to derive background-free CARS spectra with Lorentzian line shapes (Figures 2 and 3). The $\chi^{(3)}$-fitting parameters (band origins, Ω_k, bandwidths, Γ_k, and amplitudes, A_k) utilized for these PR/CARS data are presented in Table 1. The error in measuring a given band origin position is <2 cm^{-1}. The band origins for BR6.11 derived from RR[18] and for BR-570 from PR/CARS data are also included in Table 1. The comparison of PR/CARS spectra from BR6.11 (this work) and BR-570[7] (Figures 4 and 5) highlights the differences in the retinal structure and bonding attributable to the introduction of the six-membered ring bridging the C_{11}═C_{12}−C_{13} bonds.

B. Vibrational Mode Assignments for BR6.11. The normal mode assignments in BR6.11 are determined from comparisons with the analogous normal mode assignments for native BR-570. Generally, the six-membered ring can be anticipated to cause only minor perturbations to those BR-570 normal modes localized near the β-ionone ring and to cause major perturbations (e.g., create new normal modes) where the six-membered ring is directly involved in nuclear displacements (e.g., near the C_{11}═C_{12}−C_{13} bonds). Comparisons with the vibrational spectra (PR/CARS and RR) from other artificial BR pigments containing ring structures (BR6.9[20] and BR5.12[19]) are also used to facilitate the vibrational mode assignments.

1. HOOP and C−CH_3 Rocking Modes. The vibrational bands at 814 cm^{-1}, 837 cm^{-1}, 880 cm^{-1}, 889 cm^{-1} (sh), 902 cm^{-1}, 914 cm^{-1}, and 974 cm^{-1} are associated with hydrogen out-of-plane (HOOP) wagging modes in BR6.11 (Figure 4, bottom).[29,30] The HOOP bands in BR6.11 are more intense (e.g., relative to the neighboring 1165 cm^{-1} band) than the analogous HOOP bands in the native BR-570 spectrum (Figure 4), an indication of larger out-of-plane distortion in the BR6.11 chromophore.

The intense band at 1008 cm^{-1} in BR-570 is assigned primarily to in-plane rocking modes involving the C_{19} and C_{20} methyl groups (C−CH_3 rocking vibrations).[29,30] The C_{20} methyl group is absent in BR6.11 due to the presence of the six-membered ring (Figure 1). Nevertheless, a relatively intense band appearing at 1018 cm^{-1} (Figure 4) can be attributed to the single in-plane methyl-rocking mode associated with the

TABLE 1: Band Positions (Intensity Maxima for Resonance Raman (RR) and Origins, Ω_k, for CARS Data) in Vibrational Spectra Recorded from BR6.11 and BR-570, and Bandwidths, Γ_k, and Amplitudes, A_k for PR/CARS of BR6.11

BR6.11[a]					BR-570[b]	J6.11[c]	K6.11[c]
RR[d] band int. max. (cm^{-1})	PR/CARS[c,e] Ω_k (cm^{-1})[h]	PR/CARS[c,e] Γ_k (cm^{-1})[h]	PR/CARS[c,e] A_k[h,i]	vibrational mode assignments[f]	P(T)R/CARS[g] Ω_k (cm^{-1})[h]	P(T)R/CARS[g] Ω_k (cm^{-1})[j]	P(T)R/CARS[g] Ω_k (cm^{-1})[j]
	814	11	0.02	lysine (HOOP)	830		
	837	15	0.02	C_7-, C_8-H (HOOP)	850		
880	880	4	0.09	$C_{11}-$, $C_{12}-$, $C_{14}-$H (HOOP)	883	877	879
	889	5	0.02				
	902	5.5	0.05	$C_{10}-$H (HOOP)	898	905	904
	914	3.5	0.03			915	920
						918	
							947
	974	31	0.04	$C_{11}-$, $C_{12}-$H (HOOP) C_7-, C_8-H (HOOP)	959 982	978	970
							1000
1016	1018	6	0.12	CH_3 ip rock (sym.)	1008		
	1029	12.5	0.08	CH_3 ip rock (asym.)	1022	1028	1026
	1049	11	0.08	CH_3 oop rock	1048		
	1059	11	0.09				
	1077	10	0.05			1081	1076
	1098	5	0.02				
	1122	8	0.06	C_6-C_7 stretch	1122		1112
	1139	10	0.11	$\beta-$ionone ring stretch	1137		1150
1164	1165	7	0.70	$C_{10}-C_{11}$ stretch	1171	1166	1175
	1189	4	0.03		1185		1199
	1199	5	0.08	$C_{14}-C_{15}$ stretch	1202	1203	1203
1210	1214	7	0.28	C_8-C_9 stretch	1213	1213	1213
						1223	1224
	1242	6	0.02	lysine (ip rock)		1241	1239
	1246	6	0.04				
	1251	6	0.08		1254	1250	
	1272	11	0.06	$C_{11}-$H (ip rock)	1274	1269	1264
	1295	10	0.05				1297
	1308	18.5	0.05	C_7-, C_8-H (ip rock)	1306	1303	
	1311	5	0.007				
	1322	5	0.09	$C_{11}-$, $C_{12}-$, $C_{15}-$H (ip rock)	1324	1323	1322
	1335	3	0.02			1335	1336
	1348	10	0.09	N$-$H (ip rock)	1349	1345	1352
						1355	
	1368	6.5	0.04			1370	1369
	1380	5.5	0.03	CH_3 sym. deform.	1382	1380	1380
	1398	10	0.04			1400	1393
	1413	5	0.02			1416	1413
	1421	6	0.05			1430	1426
	1435	7	0.03			1439	
	1450	8	0.02	CH_3 ip deform.	1456	1451	1449
	1459	33	0.09				
	1466	8	0.002			1468	1469
	1488	5	0.01				1485
1510	1510	7	1.000	$C_{11}=C_{12}$ stretch	1526	1508	1512
	1545	10	0.09				
				$C_{13}=C_{14}$ stretch	1580	1574	1576
1589	1593	11	0.06	$C_7=C_8$ stretch	1601	1586	1586
							1618
	1647	11	0.05	C=N stretch	1638	1637	1651
	1690	3	0.01			1669	1674

[a] Refs 14, 15. [b] Ref 7. [c] This work. [d] Resonance Raman data.[18] [e] PR/CARS = picosecond resonance coherent anti-Stokes Raman scattering. [f] Based on comparisons with assignments of RR data from BR-570.[30] Only the predominant local coordinates characterizing each normal mode are shown (ip = in-plane, oop = out-of-plane and HOOP = hydrogen out-of-plane). [g] Picosecond time-resolved CARS (PTR/CARS, J6.11 and K6.11) or PR/CARS (BR-570). [h] Derived from $\chi^{(3)}$ fit of PR/CARS data. [i] Relative intensities obtained by normalization to the most intense feature at 1510 cm^{-1}. [j] Derived from $\chi^{(3)}$ fit of PTR/CARS data.

C_{19} methyl group. This assignment is consistent with those made for the analogous bands in BR5.12 (at 1020 cm^{-1} for the C_{19} and C_{20} methyl rocking modes)[19] and in BR6.9 (at 1017 cm^{-1} for the C_{20} methyl rocking mode).[20]

The relatively weak 1048 cm^{-1} band in BR-570 is assignable to out-of-plane C_{19} and C_{20} methyl rocking modes.[29,30] By analogy with this and similar bands appearing in the spectra for BR6.9 (1051 cm^{-1}) and BR5.12 (1050 cm^{-1}), the 1059 cm^{-1} band in the BR6.11 spectrum is assigned to the C_{19} methyl out-of-plane rocking mode. In the BR6.11 spectrum, however, this band appears with a relatively larger intensity than the analogous bands for the other BR pigments, an indication of a significantly larger degree of out-of-plane displacement of the C_{19} methyl in BR6.11.

The peaks in the 1274$-$1456 cm^{-1} region of the BR-570 spectrum (Figure 5) are assigned mainly to hydrogen in-plane rocks (e.g., 1274 cm^{-1}, 1306 cm^{-1}, and 1324 cm^{-1}) as well as in-plane and out-of-plane methyl deformations (e.g., 1382 cm^{-1} and 1456 cm^{-1}). Overall, the positions and relative intensity pattern in this region of the BR6.11 spectrum (Figure 5) is

significantly different than that observed for BR-570. Of particular interest is the 1349 cm^{-1} band in BR-570 that is assigned to the N−H (Schiff base hydrogen) in-plane rock.[29,30] The spectral changes seen in this region of the BR6.11 spectrum recorded in D_2O are consistent with its 1348 cm^{-1} band being assigned to the N−H in-plane rocking mode (data not shown).

2. C−C Stretching Modes. The pattern of vibrational bands in the C−C stretching "fingerprint" region (∼1120−1220 cm^{-1}) is slightly different in BR6.11 than in the native BR-570 (Figure 4). The fingerprint bands are assigned to modes involving predominantly C−C stretching motions that are strongly coupled to in-plane C−C−H rocking motions.[29−31] These C−C stretching bands are used to identify the isomeric configuration of retinal as either all-trans or 13-cis.[8,28,31]

In the fingerprint region of the BR6.11 spectrum, six peaks are identified at 1122 cm^{-1}, 1139 cm^{-1}, 1165 cm^{-1}, 1189 cm^{-1} (weak), ∼1199 cm^{-1} (weak shoulder), and 1214 cm^{-1} (Figure 4). The most intense peak at 1165 cm^{-1} can be assigned to the vibrational mode having predominantly $C_{10}-C_{11}$ stretching character, with some coupling to the $H-C_{10}-C_{11}$ rocking motion, by analogy with the intense band appearing at 1171 cm^{-1} in BR-570,[27,30] 1171 cm^{-1} in BR6.9[20] and 1182 cm^{-1} in BR5.12.[19]

The two intense bands at 1202 cm^{-1} and 1213 cm^{-1} in BR-570 are assigned to the strongly coupled $C_{14}-C_{15}$ and C_8-C_9 stretching modes.[30] In BR6.11, the bands at 1214 cm^{-1} and with a weak shoulder at ∼1199 cm^{-1} are likely associated with these modes. The aliphatic ring in the retinal of BR6.11 thus greatly affects the intensity of these bands, but not their positions. The reduced intensities may be attributed to the altered coupling between the C_8-C_9 and $C_{14}-C_{15}$ stretches, due to the ring bridging the $C_{11}=C_{12}-C_{13}$ carbons between them.

3. C=C Stretching and Schiff-base Modes. The PR/CARS spectrum of BR6.11 contains one major, intense band at 1510 cm^{-1} and two other bands at 1545 cm^{-1} and 1593 cm^{-1}, all of which are attributed to C=C stretching (ethylenic) modes (Figure 5). Although normal coordinate analyses indicate that the C=C stretches in retinal are strongly coupled,[29−31] the most intense band in BR-570 (at 1526 cm^{-1}) and that of BR6.11 (1510 cm^{-1}) is assigned predominantly $C_{11}=C_{12}$ stretching character. The band at 1647 cm^{-1} (1622 cm^{-1} in D_2O, data not shown) in the BR6.11 spectrum is assigned to the C=N stretching mode associated with the protonated Schiff-base linkage to the Lys216 residue of opsin.[8,19,29−31] This is a higher frequency than that found in BR-570 (1638 cm^{-1}),[27] BR6.9 (1640 cm^{-1})[20] and BR5.12 (1631 cm^{-1}).[19]

II. BR6.11 Photocycle Intermediates. PTA data (not shown) measured over the initial 250 ps of the BR6.11 room temperature photocycle (570 nm pump and 663 nm probe wavelengths) identify two intermediates, J6.11 and K6.11, both of which have previously been reported.[14] A global fit of the PTA data yields a 16 ± 4 ps time constant for the decay of J6.11 that agrees with previous findings (12 ± 3 ps).[14] The lifetime of the K6.11 species is >1 μs.

Previous PTA measurements of BR6.11 revealed the presence of two discernible K6.11 species, denoted K6.11/1 and K6.11/2, each with a lifetime of ∼100 ps and ≫5 ns, respectively.[14] However, no evidence of a ∼100 ps K6.11 intermediate is found in the present PTA data. The absence of such an intermediate is supported by the PTR/CARS data, which reveal no structural changes beyond ∼30 ps throughout the 0−250 ps time interval studied, vide infra.

A. PTR/CARS Spectrum of K6.11. PTR/CARS spectra are recorded at 5 ps intervals throughout the initial 200 ps of the BR6.11 photocycle, using the simultaneously recorded PTA signals to quantitatively determine the absolute time scale as well as the delay intervals. Attention is focused on the vibrational spectrum of K6.11 that has a relatively long lifetime (>1 μs). The resultant background-free CARS spectrum of K6.11 (800−1700 cm^{-1}), derived from the PTR/CARS spectrum recorded at 200 ps, is presented in two spectrally overlapped regions, each spanning ∼500 cm^{-1} (bottom of Figures 6 and 7). The same background-free CARS spectrum of K6.11 is obtained from each independent PTR/CARS measurement between 30 and 200 ps (data not shown), all delay times at which the concentration of K6.11 is seen from the PTA data to be almost constant. To facilitate comparisons, the background-free CARS spectrum of BR6.11 is presented at the top of Figures 6 and 7.

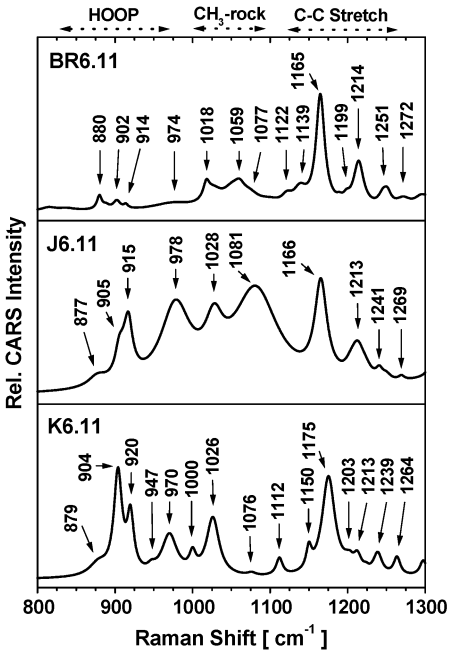

Figure 6. (Top) Background-free (Lorentzian line shapes) PR/CARS spectrum of BR6.11 and PTR/CARS spectra of J6.11 (center, derived from the 0-ps PTR/CARS data) and K6.11 (bottom, derived from the 200-ps PTR/CARS data) in the 800−1300 cm^{-1} region. Band positions are origin (Ω_k) values derived from $\chi^{(3)}$ fits of the PR/CARS and PTR/CARS data (Table 1). The spectral regions corresponding to hydrogen out-of-plane (HOOP), methyl-rocking (CH_3-rock), and C−C stretching vibrational modes are indicated at the top of the figure (dotted lines).

B. Vibrational Mode Assignments for K6.11. The appearance of the same 800−1700 cm^{-1} bands in PTR/CARS spectra recorded between 30 and 200 ps delays demonstrates that K6.11 is an intermediate with well-defined vibrational modes over the entire 30−200 ps time interval. Independently, the differences in the PTR/CARS spectrum assigned to K6.11 and the PR/CARS spectrum of BR6.11 (Figures 6 and 7) demonstrate that the respective retinal structures are themselves distinct.

1. HOOP and CH_3-rocking Modes. The vibrational bands for K6.11 appearing at 879 cm^{-1}, 904 cm^{-1}, 920 cm^{-1}, 947 cm^{-1}, and 970 cm^{-1} are assigned to HOOP modes. Of particular note is the marked increase in the relative intensity and bandwidth of these modes in comparison with the analogously assigned bands in the BR6.11 spectrum (Figure 6). Both characteristics indicate that the polyene chain in K6.11 is significantly more twisted and/or distorted out-of-plane than that in BR6.11. The 1018 cm^{-1} band, corresponding to in-plane methyl rocking motion in BR6.11, is similarly more intense and broadened in the K6.11 spectrum (1026 cm^{-1} band). The weak band appear-

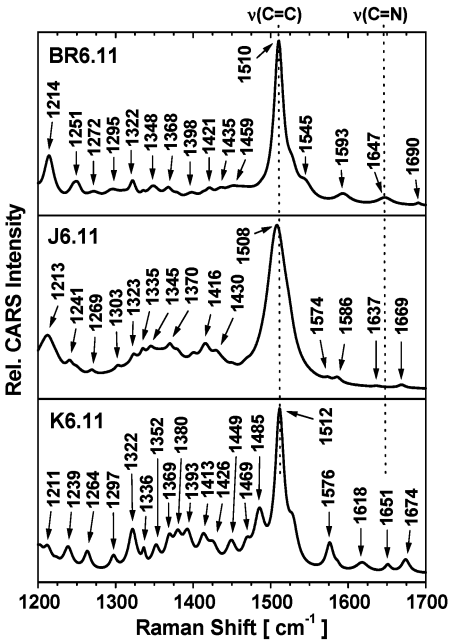

Figure 7. (top) Background-free (Lorentzian line shapes) PR/CARS spectrum of BR6.11 and PTR/CARS spectrum of J6.11 (center, derived from the 0-ps PTR/CARS data) and K6.11 (bottom, derived from the 200-ps PTR/CARS data) in the 1200−1700 cm^{-1} region. Band positions are origin (Ω_k) values derived from the $\chi^{(3)}$ fits of the PR/CARS and PTR/CARS data (Table 1).

ing at 1076 cm^{-1} in the K6.11 spectrum is assignable to an out-of-plane methyl rocking mode.

2. C−C Stretching Modes. The general pattern of vibrational bands in the C−C stretching (fingerprint) region of the K6.11 spectrum is substantially different than that found in BR6.11, with respect to both the relative intensities and band positions (Figure 6). The most intense band appears at 1175 cm^{-1} and is broadened relative to the intense 1165 cm^{-1} band in the BR6.11 spectrum. Assuming that these bands are associated with the same vibrational mode, the 10 cm^{-1} increase in the frequency in K6.11 is indicative of greater force constant(s) associated with these degrees of freedom (i.e., mainly the $C_{10}-C_{11}$ stretching mode coupled with $C_{10}-H$ in-plane rock). The significantly weaker relative intensity of the band at 1213 cm^{-1} in K6.11 (1214 cm^{-1} in BR6.11) indicates further decoupling of the C_8-C_9 and $C_{14}-C_{15}$ stretches in K6.11 (vide supra). The second major C−C stretching band, associated with the $C_{14}-C_{15}$ mode, appears only as a weak shoulder at ∼1203 cm^{-1} in the K6.11 spectrum. Collectively, these C−C stretching bands demonstrate that the incorporation of a six-membered aliphatic carbon ring bridging the $C_{11}=C_{12}-C_{13}$ bonds does not prevent the appearance of significant out-of-plane twisting/distortion in K6.11, which has a 13-cis retinal configuration (vide infra).

3. C═C stretching and Schiff-base Modes. The vibrational band patterns in the C═C stretching and Schiff-base regions differ significantly between BR6.11 and K6.11. Although the position of the most intense BR6.11 band at 1510 cm^{-1}, assigned to the predominantly $C_{11}=C_{12}$ stretching mode, shifts only slightly to 1512 cm^{-1} in K6.11, it is accompanied by the emergence of another moderately intense band at 1485 cm^{-1} (Figure 7). The very weak band at 1651 cm^{-1} is tentatively assigned to the C═N stretching mode, 4 cm^{-1} higher than that in BR6.11.

C. PTR/CARS Spectrum of J6.11. Although the visible absorption spectra of BR6.11, J6.11, and K6.11 overlap extensively, the presence of J6.11 in the BR6.11 photocycle, as well as its 12−16 ps lifetime, is clearly evident from the PTA data.[14] The measurement of the vibrational spectra of J intermediates, in general, is made difficult by their short lifetime relative to the ∼3−5 ps laser pulse widths needed to obtain vibrational data with spectral bandwidths consistent with assigning normal modes (i.e., obtaining structural information). Nevertheless, recording the PTR/CARS spectrum of an intermediate with a lifetime as short as 3 ps (e.g., J-625 in the BR-570 photocycle) is feasible if the relative concentrations of the species present during the CCT can be determined. Such data are obtained from PTA experiments. For example, since PTA measurements show that the concentrations of both I-460 and K-590 are insignificant within a CCT of 6.5 ps, the resultant PTR/CARS spectra can be quantitatively analyzed in terms of only J-625 and BR-570. The vibrational spectrum of J-625 alone can be determined by incorporating the well-established CARS spectrum of BR-570 into the third-order susceptibility fitting function for the PTR/CARS data.[7]

The same methodology is used to obtain the vibrational CARS spectrum of J6.11 in the BR6.11 photocycle (Figures 6 and 7). The 12−16 ps lifetime of J6.11 makes it experimentally feasible to record several PTR/CARS spectra having measurable J6.11 contributions at different time delays (e.g., from 0 to 10 ps). These independently measured vibrational spectra of J6.11 are themselves consistent and distinct from those of BR6.11 and K6.11.

The most distinctive characteristic of the CARS spectrum assigned to J6.11 is the large, exceptionally broad (∼200 cm^{-1}) feature appearing in the low-frequency HOOP and CH_3-rocking regions (877−1081 cm^{-1}, Figure 6). Such a broad, intense feature indicates that the retinal has a large degree of out-of-plane motion that has not organized into specific nuclear motions well described by normal modes. The disappearance of the ∼200 cm^{-1} broad feature during the J6.11 to K.11 transformation reflects the time dependent nature of the out-of-plane motion as it relaxes into HOOP and CH_3-rocking normal modes. Since the pattern of C−C stretching bands of J6.11 (1166 and 1213 cm^{-1}) closely resembles that observed for BR6.11, but is distinct from that of K6.11 (Figure 6), it is evident that the retinal has isomerized in the transformation from J6.11 to K6.11. Significant structural changes in the retinal have occurred as J6.11 is formed, however, such as the out-of-plane twisting/distortion shown by the strong HOOP and CH_3-rocking bands (Figure 6).

The intense bands in the C═C stretching regions are also similar for BR6.11 and J6.11, although small displacements (1510 cm^{-1} in BR6.11 to 1508 cm^{-1} in J6.11) and significant broadening in J6.11 are observed (Figure 7). This similarity suggests that the electron delocalization along the polyene chain does not change much between BR6.11 and J6.11, a conclusion supported by the small shifts (∼2 cm^{-1}) found for all the positions of the C−C and C═C bands in J6.11 (i.e., 1166, 1213, and 1508 cm^{-1}) relative to the corresponding BR6.11 bands.

Discussion

The measurement of changes in retinal structure occurring within the initial 200 ps of the BR6.11 photocycle, as determined from the PR/CARS and PTR/CARS data presented here (Figures 2−7), provides an opportunity to expand the primarily kinetic models of BR photoreactivity (derived from transient absorption data) to include an understanding of the structural dynamics of the retinal chromophore. These initial structural transformations involve the J6.11 and K6.11 intermediates and reflect differences in both retinal configurations and conformations and in the interaction(s) between retinal and the amino acid residues

compising the protein binding pocket. Comparisons of the retinal dynamics in BR6.11 with those in the photocycles and photoreactions of native BR-570[7,8] and other artificial BR pigments[19,20] further expand the understanding of the molecular events that characterize the photoreactivity of BR in general.

A. Structure of BR6.11. PR/CARS data (Figures 4 and 5) show that, in general, the modifications to the retinal caused by the incorporation of a six-membered carbon ring spanning the C_{11}═C_{12}−C_{13} bonds to form BR6.11 are relatively small. Many similar vibrational features are observed in both the PR/CARS spectra of BR-570 and BR6.11. Because normal coordinate calculations, selected ^{13}C isotopic substitutions and bleaching/chromatographic studies[30−32] together have identified the C−C stretching band pattern observed from BR-570 as originating from an all-trans retinal, the overall similarity of the C−C stretching band patterns in BR-570 and BR6.11 (Figure 4) specifically supports the conclusion of earlier bleaching/chromatographic studies[15] that light-adapted BR6.11 also contains an all-*trans* retinal. Detailed examination of these PR/CARS spectra, however, reveals several noteworthy differences in the retinal structures of BR6.11 and BR-570:

1. The enhanced intensity of the HOOP and C−CH_3 out-of-plane rocking modes in the BR6.11 spectrum (e.g., 880 cm^{-1} and 1059 cm^{-1}, Figure 4) can be attributed to steric interactions of the ring with surrounding amino acid residues in the protein pocket, which cause increased out-of-plane distortion of the retinal. The most likely retinal/amino acid interactions involve Trp182 and Leu93 (the X-ray crystal structure of BR-570 shows the C_9−CH_3 and C_{13}−CH_3 groups to be 3.6 and 3.7 Å, respectively, from the closest heavy atom in Trp182 and Leu93).[33,34] Because these residues are likely contact points between the retinal and the protein, the replacement of the C_{13}−CH_3 group by the six-membered ring in BR6.11 is expected to create the strong interaction (contact?) with Trp182 and Leu93 needed to alter the retinal conformation relative to the protein binding pocket. The increased intensity of the C_9−CH_3 out-of-plane rocking band observed in the PR/CARS spectrum of BR6.11 (1059 cm^{-1}, Figure 4) results from such altered steric interaction (i.e., forcing the C_9−CH_3 group out of the plane defined by the polyene backbone).

2. The significantly lower (∼16 cm^{-1}) position of the strong C═C stretching band (1510 cm^{-1}) in BR6.11 (Figure 5) can be associated with increased pi-electron delocalization throughout the retinal introduced by the incorporation of the aliphatic carbon ring, an effect found in other artificial BR pigments (e.g., BR5.12[19] and BR6.9[20]). Although the C_{11}═C_{12} stretching mode makes the major contribution to 1510 cm^{-1} band intensity,[30] significant contributions are made by other C═C stretching modes and minor contributions are made by several C−C stretches and C−H in-plane rocking modes.[30] The ethylenic character of the mode, however, dominates and underlies its sensitivity to the degree of pi-electron delocalization along the polyene backbone. The perturbation of the ring on the pi-electron density originates from its interaction with Trp182 in the protein binding pocket (vide supra).

3. The higher frequency of the C═N stretching band in BR6.11 (1647 cm^{-1}, Figure 5) suggests a change in retinal conformation in the Schiff base region (Figure 1). The strong coupling between the C═N stretching mode and the N−H rock of the Schiff base[30] causes the C═N bond frequency to be greatly influenced by the hydrogen bonding characteristics of the Schiff base, which itself reflects its interactions with the surrounding protein. In BR-570, the Schiff base interacts with Asp85 via a hydrogen-bonding bridge involving at least one water molecule (w402).[34] In artificial pigments (e.g., BR6.11), the hydrogen-bonding is anticipated to be different because the orientation of the artificial retinal within the protein pocket is altered, vide supra. For example, increasing the distance to Asp85 weakens the Schiff base hydrogen-bond with w402, increases the coupling between the N−H rock and the C═N stretching modes, and increases the C═N stretching frequency.[32] Alternatively, the degree of pi-electron delocalization along the polyene chain can influence the frequency of the C═N stretch (e.g., decreased pi-electron delocalization near the Schiff base increases the C═N stretching frequency). Because the C═C stretching frequency indicates that pi-electron delocalization increases in BR6.11, the increase in the frequency of the C═N stretching band is attributable to a weakening of the Schiff base hydrogen-bonding to Asp85.

B. Retinal Structural Dynamics in the BR6.11 Photocycle. The molecular mechanism occurring within the initial 200 ps of the BR6.11 photocycle can now be characterized in terms of both PTA data reflecting changes in the electronic states populated and CARS data measuring the changes in vibrational degrees of freedom. While PTA data establish the kinetic properties of two distinct intermediates, J6.11 and K6.11, the PTR/CARS data presented here (Figures 6 and 7) provide insight into their respective retinal structures relative to that of BR6.11. Thus, a dynamical model for the initial 200 ps of the BR6.11 photocycle based on both structurally and kinetically characterized intermediates can be constructed. Comparisons of this dynamical model with those based on analogous CARS data from the photoreactions in native BR and other artificial BR pigments also provide an understanding of the initial reaction coordinates in BR systems in general.

J6.11. The absence of significant changes in the C−C stretching band pattern upon J6.11 formation from BR6.11 shows that no C═C isomerization has taken place, and therefore, that intense, delocalized out-of-plane motion in J6.11 occurs within an all-trans-like retinal configuration and that C═C isomerization is not a primary reaction coordinate in the formation of J6.11.

While the intense, delocalized, out-of plane motions in the HOOP and C−CH_3 rock regions appearing in the PTR/CARS spectra from both J-625 and J6.11 (Figure 8) are generally similar, a detailed comparison reveals a noteworthy difference: the intensity maximum of the broad, delocalized, out-of-plane feature appears in the 800−900 cm^{-1} HOOP region in J-625, while the intensity maximum increases into the 1000−1100 cm^{-1} CH_3 rocking region in J6.11 (Figure 8). The ∼200 cm^{-1} difference can be attributed to the restricted motion within the retinal and/or the alteration of the retinal interactions with the surrounding amino acid residues of the protein. In the first case, out-of-plane motion in any of the C_6−C_7═C_8−C_9═C_{10}−C_{11} and C_{13}═C_{14}−C_{15}═N bonds left unrestricted in BR6.11 could contribute to the broad spectral feature observed (Figure 8). Alternatively, having the CH_3 groups assume different positions relative to the nearby Trp182 and Leu93 residues (i.e., C_{20}−CH_3 is absent and C_{19}−CH_3 is moved in BR6.11) likely changes the degree of out-of-plane flexibility within the retinal. In either case, the frequency of the delocalized out-of-plane motion depends directly on flexibility of specific C−C═C polyene bonds, which can be controlled by incorporating a carbon ring into a specific retinal location.

Most significantly, however, the ring bridging the C_{11}═C_{12}−C_{13} bonds of the BR6.11 retinal does not prevent the appearance of an intense, broad, delocalized, out-of-plane feature in J6.11, even though it shifts its intensity maximum. A comparison of

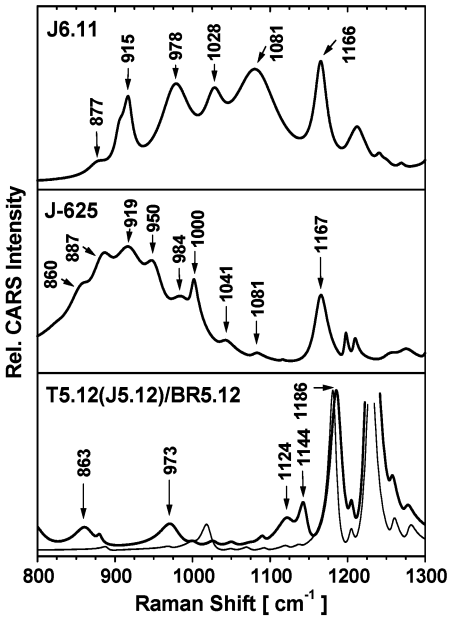

Figure 8. (Top) Background-free (Lorentzian line shapes) PTR/CARS spectrum of J6.11 (derived from the 0-ps PTR/CARS data, this work), PTR/CARS spectra of J-625 (center)[7] and T5.12(J5.12) (Bottom, thick line)[19] and PR/CARS spectrum of BR5.12 (Bottom, thin line)[19] in the 800−1300 cm^{-1} region. The T5.12(J5.12) and BR5.12 spectra are normalized with respect to the C−C stretching band at 1186 cm^{-1} in the T5.12(J5.12) spectrum (1182 cm^{-1} in the BR5.12 spectrum[19]). Band positions are origin (Ω_k) values derived from $\chi^{(3)}$ fits of the PTR/CARS data (Table 1).

PTR/CARS spectra (Figure 8) from J6.11, J-625, and T5.12-(J5.12) ($C_{12}-C_{13}=C_{14}$ bonds locked in a 13-trans retinal, Figure 1) reveals a second type of enhanced out-of-plane motion. Although no intense, broad (∼200 cm^{-1}) feature appears in T5.12(J5.12), its HOOP bands (863 cm^{-1} and 973 cm^{-1}) are measurably more intense and broader than those in the BR5.12 spectrum (bottom, Figure 8), an observation attributable to the restricted motion in the $C_{12}-C_{13}=C_{14}$ bonds introduced by the five-membered ring (Figure 1). Collectively, these CARS data suggest that the delocalized out-of-plane motion involves bonds primarily in the Schiff base ($C_{12}-C_{13}=C_{14}-C_{15}=N$) region. This conclusion is consistent with theoretical calculations indicating that out-of-plane motion eventually localizes in the Schiff base region of the retinal upon the formation of K-590.[12]

K6.11. The narrowed and decreased intensity of the HOOP and $C-CH_3$ rocking bands in K6.11 (Figure 6) indicate that retinal relaxes toward a more planar, less twisted configuration during its formation from J6.11. An analogous relaxation is observed in the formation of K-590 from J-625 in the native BR photocycle.[7,8] The retinal in K6.11, however, remains more distorted than K-590[7,11,12,28] (Figure 6), an observation likely related to steric interactions of the ring in BR6.11 with the protein pocket that hinders a more planar retinal configuration from forming. (A similar steric hindrance may also affect the J6.11 to K6.11 transformation rate, vide infra.)

In contrast to the J6.11 case, a distinctly different C−C stretching band pattern appears in the K6.11 spectrum (Figure 6), showing that the retinal configuration has changed during the J6.11 to K6.11 transformation. Several vibrational mode assignments made in previous BR studies indicate that isomerization occurs specifically at the $C_{13}=C_{14}$ bond: (i) $C_{11}=C_{12}$ isomerization is prevented by the ring in BR6.11, (ii) $C_9=C_{10}$ isomerization is characterized by a significant *decrease* in the $C_{10}-C_{11}$ stretching band position[32] which contrasts the 10 cm^{-1} *increase* in this band position in K6.11 (Figure 6), and (iii) an increase in the $C_{10}-C_{11}$ band position is assigned specifically to a 13-cis retinal.[32] When combined with the bleaching/chromatographic data showing that the BR6.11 photocycle eventually generates a 13-cis retinal,[15,21] these spectroscopic results strongly support the conclusion that K6.11 contains a 13-cis retinal and that $C_{13}=C_{14}$ isomerization occurs during the transformation from J6.11 to K6.11.

Dynamical Model for the BR6.11 Photocycle. The significantly slower rate ($\tau \sim 12-16$ ps) for the J to K transformation in BR6.11 relative to that in BR-570 (3.5 ps[6,16,17]) directly reflects the time required for trans to cis isomerization of the $C_{13}=C_{14}$ bond. The decreased isomerization rate in BR6.11 arises from the proximity of the ring to the $C_{13}=C_{14}$ bond, which increases inertia near the $C_{13}=C_{14}$ bond and introduces new steric interactions between the ring and amino acid residues. As a consequence, the rate at which torsional motion is converted into isomerization of the $C_{13}=C_{14}$ bond slows.

While trans to cis isomerization of the $C_{13}=C_{14}$ bond in retinal remains a picosecond molecular event critical to the initiation of the BR photocycle (i.e., trans-membrane proton pumping), changes in the out-of-plane motions precede $C_{13}=C_{14}$ isomerization and therefore, comprise the reaction coordinates that prepare retinal for $C_{13}=C_{14}$ isomerization. These out-of-plane degrees of freedom are observed as "primary" reaction coordinates in not only the CARS data presented here for BR6.11, but for those data observed previously for BR-570 and BR5.12.

Both two-[1,6] and three-state[35,36] dynamical models have been considered in the description of the initial molecular events in the BR photocycle. Two-state models incorporate optical excitation to an excited electronic state that is repulsive along the $C_{13}=C_{14}$ torsional coordinate, leading directly to $C_{13}=C_{14}$ isomerization following photoexcitation.[1,6] Three-state models[35,36] incorporate a potential energy barrier on the excited electronic state potential surface (along the $C_{13}=C_{14}$ torsional coordinate) reached by photoexcitation, and therefore, following photoexcitation, $C_{13}=C_{14}$ isomerization occurs only after a barrier crossing. In general, the excited electronic state trajectory(ies) leading to barrier crossing may involve a variety of internal retinal coordinates including that along the $C_{13}=C_{14}$ torsional coordinate. Whichever coordinates are involved, however, they must facilitate the barrier crossing leading to $C_{13}=C_{14}$ isomerization. The CARS data presented here, and previously,[7,19,20] indicate that the out-of-plane motions observed in J-like intermediates act as the primary reaction coordinates by which the excited electronic state potential barrier is crossed. It is well established that out-of-plane motion along a polyene chain shifts the relative energies and mixes the vibronic symmetries of excited electronic states,[37] both of which can facilitate the lowering of energy barriers and create curve crossings among excited electronic states. Thus, the CARS data presented here showing that out-of-plane motion (i.e., twisting of the polyene chain in retinal) is a precursor to $C_{13}=C_{14}$ bond isomerization support a three-state model description of the primary (<50 ps) events following photoexcitation in BR pigments.

The important role of out-of-plane motion as a precursor to $C_{13}=C_{14}$ isomerization is not in agreement with recently published interpretations of a pump−probe (femtosecond), infrared absorption study.[38] Specifically, the intensity of the 1190 cm^{-1} infrared absorption band assigned to the C−C stretching mode in K-590[7,8,28] is reported to increase on the femtosecond time scale.[38] Because K-590 is viewed as having a 13-cis retinal, the increase of the 1190 cm^{-1} band intensity on a time scale

comparable to the 500 fs lifetime of J-625[6] is interpreted as showing that J-625 also has a 13-cis retinal. This conclusion, however, needs to be considered with caution. The ~200 fs pulse-width of the infrared probe laser used in these experiments[38] generates such a broad (~60 cm^{-1}) spectral bandwidth for monitoring absorption changes that it makes it difficult to resolve any single vibrational band or mode. Thus, assigning the changes in infrared absorption intensity to a specific retinal mode (e.g., C−C stretching) is correspondingly difficult. The observed intensity increase reported could be attributable to any one of several modes assigned to be within the ~60 cm^{-1} region covered by the probe pulse. By contrast, the PTR/CARS spectra presented here for BR6.11, and previously for BR-570[7] and other artificial BR pigments, contain all the time-dependent bands within the entire C−C ("fingerprint") region (spectral resolution of ~2 cm^{-1}) and therefore, a comprehensive series of mode assignments can be made.

Finally, the electronic state properties of J intermediates in general, and J6.11 specifically, remain important issues to be established. The three-state model depicts the J intermediate to be in the excited electronic state with a distorted (≤90°) C_{13}═C_{14} torsional bond angle (similar to the "tumbling state" described previously[39]). The observations of significant band broadening in J intermediates (e.g., Figures 6 and 7 this work and Figure 4 of ref. 7) also supports its assignment as an excited electronic state.

In the native BR photocycle, the stimulated emission expected from an excited electronic state is observed from I-460,[23] but not from J-625. Thus, if J-625, and by analogy J6.11, is an excited electronic state, stimulated emission to the A_g ground state of retinal must be highly forbidden. This circumstance obtains if J intermediates also have A_g electronic symmetry. Since the initial optical excitation of BR populates a B_u (Franck−Condon) electronic state and I-460 appears to maintain a B_u character (based on its observed stimulated emission[23]), the formation of J-625 as an A_g electronic state from I-460 requires a symmetry change. Such a B_u to A_g symmetry transition is consistent with a three-state model in which the barrier separating the Franck−Condon region of the potential (populated optically) arises from an avoided crossing involving the two lowest excited electronic states with B_u and A_g character.

The ground electronic state (A_g) nature of K-590 is determined from the X-ray crystal structure recorded from a cryogenically trapped K-590 sample.[11] As anticipated for a ground state species, fluorescence from K-590 is observed only following photoexcitation.[40,41] Vibrational spectra (time-resolved RR and PTR/CARS) show that K-590 (and by analogy K6.11) maintains a well-defined, 13-cis retinal structure throughout its 1−2 μs lifetime.[7,28] Thus, ground-state K-590 appears only after a B_u to A_g curve-crossing and corresponding C_{13}═C_{14} isomerization.

Importantly, the out-of-plane motions found to comprise the primary reaction coordinates assignable to J intermediates drive the excited electronic state curve crossing by mixing B_u and A_g electronic character. A model for the initial stages of the BR photoreaction that incorporates out-of-plane retinal motion as the primary reaction coordinate is consistent with both the electronic state absorption and emission data as well as with the vibrational spectroscopic data characterizing individual intermediates.

Acknowledgment. The authors thank Dr. Mudi Sheves (Department of Organic Chemistry, Weizmann Institute, Israel) and Dr Michael Ottolenghi (Department of Chemistry, Hebrew University, Israel) for providing the Ret6.11 chromophore and for many helpful discussions. We also wish to express our appreciation to Dr. Halina Abramczyk (Technical University of Lodz, Poland) for discussions throughout the preparation of this manuscript. This research was supported through grants to G.H.A. from the National Institutes of Health and the National Science Foundation. L.U. and AT gratefully acknowledge financial support from Innovative Lasers Corporation.

References and Notes

(1) Mathies, R. A.; Lin, S. W.; Ames, J. B.; Pollard, W. T. *Annu. Rev. Biophys. Biophys. Chem.* **1991**, *20*, 491.
(2) Lanyi, J. K. *Int. Rev. Cytol.* **1999**, *187*, 161.
(3) Oesterhelt, D.; Tittor, J. *Trends Biochem. Sci.* **1989**, *14*, 57.
(4) Subramaniam, S.; Henderson, R. *Nature* **2000**, *406*, 653.
(5) Lanyi, J. K.; Luecke, H. *Curr. Opin. Struct. Biol.* **2001**, *11*, 415.
(6) Mathies, R. A.; Brito Cruz, C. H.; Pollard, W. T.; Shank, C. V. *Science* **1988**, *240*, 777.
(7) Atkinson, G. H.; Ujj, L.; Zhou, Y. *J. Phys. Chem. A* **2000**, *104*, 4130.
(8) Doig, S. J.; Reid, P. J.; Mathies, R. A. *J. Phys. Chem.* **1991**, *95*, 6372.
(9) Schobert, B.; Cupp-Vickery, J.; Hornak, V.; Smith, S.; Lanyi, J. *J. Mol. Biol.* **2002**, *321*, 715.
(10) Matsui, Y.; Sakai, K.; Murakami, M.; Shiro, Y.; Adachi, S.; Okumura, H.; Kouyama, T. *J. Mol. Biol.* **2002**, *324*, 469.
(11) Edman, K.; Nollert, P.; Royant, A.; Belrhali, H.; Pebay-Peyroula, E.; Hajdu, J.; Neutze, R.; Landau, E. M. *Nature* **1999**, *401*, 822.
(12) Hayashi, S.; Tajkhorshid, E.; Schulten, K. *Biophys. J.* **2002**, *83*, 1281.
(13) Tajkhorshid, E.; Baudry, J.; Schulten, K.; Suhai, S. *Biophys. J.* **2000**, *78*, 683.
(14) Brack, T. L.; Delaney, J. K.; Atkinson, G. H.; Albeck, A.; Sheves, M.; Ottolenghi, M. *Biophys. J.* **1993**, *65*, 964.
(15) Albeck, A.; Friedman, N.; Sheves, M.; Ottolenghi, M. *J. Am. Chem. Soc.* **1986**, *108*, 4614.
(16) Dobler, J.; Zinth, W.; Kaiser, W.; Oesterhelt, D. *Chem. Phys. Lett.* **1988**, *144*, 215.
(17) Nuss, M. C.; Zinth, W.; Kaiser, W.; Kölling, E.; Oesterhelt, D. *Chem. Phys. Lett.* **1985**, *117*, 1.
(18) Delaney, J. K.; Brack, T. L.; Atkinson, G. H.; Ottolenghi, M.; Friedman, N.; Sheves, M. *J. Phys. Chem.* **1993**, *97*, 12416.
(19) Ujj, L.; Zhou, Y.; Sheves, M.; Ottolenghi, M.; Ruhman, S.; Atkinson, G. H. *J. Am. Chem. Soc.* **2000**, *122*, 96.
(20) Atkinson, G. H.; Zhou, Y.; Ujj, L.; Aharoni, A.; Sheves, M.; Ottolenghi, M. *J. Phys. Chem. A* **2002**, *106*, 3325.
(21) Fang, J. M.; Carriker, J. D.; Balogh-Nair, V.; Nakanishi, K. *J. Am. Chem. Soc.* **1983**, *105*, 5162.
(22) Delaney, J. K.; Brack, T. L.; Atkinson, G. H.; Ottolenghi, M.; Steinberg, G.; Sheves, M. *Proc. Natl. Acad. Sci. U.S.A.* **1995**, *92*, 2101.
(23) Ye, T.; Friedman, N.; Gat, Y.; Atkinson, G. H.; Sheves, M.; Ottolenghi, M.; Ruhman, S. *J. Phys. Chem. B* **1999**, *103*, 5122.
(24) Oesterhelt, D.; Stoeckenius, W. *Proc. Natl. Acad. Sci. U.S.A.* **1973**, *70*, 2853.
(25) Ujj, L.; Jager, F.; Atkinson, G. H. *Biophys. J.* **1998**, *74*, 1492.
(26) Ujj, L.; Atkinson, G. H. Coherent Anti-Stokes Raman Spectroscopy. In *Handbook of Vibrational Spectroscopy*; Chalmers, J. M., Griffiths, P. R., Eds.; John Wiley and Sons Ltd.: Chichester, 2002; Vol. 1, p 585.
(27) Ujj, L.; Volodin, B. L.; Popp, A.; Delaney, J. K.; Atkinson, G. H. *Chem. Phys.* **1994**, *182*, 291.
(28) Ujj, L.; Jager, F.; Popp, A.; Atkinson, G. H. *Chem. Phys.* **1996**, *212*, 421.
(29) Smith, S. O. Resonance Raman Studies on the Mechanism of Proton Translocation by Bacteriorhodopsin's Retinal Chromophore, Ph.D. Thesis, University of California, 1985.
(30) Smith, S.; Braiman, M. S.; Myers, A. B.; Pardoen, J. A.; Courtin, J. M. L.; Winkel, C.; Lugtenburg, J.; Mathies, R. A. *J. Am. Chem. Soc.* **1987**, *109*, 3108.
(31) Smith, S.; Pardoen, J. A.; Lugtenburg, J.; Mathies, R. A. *J. Phys. Chem.* **1987**, *91*, 804.
(32) Mathies, R. A.; Smith, S. O.; Palings, I. Determination of Retinal Chromophore Structure in Rhodopsins. In *Biological Applications of Raman Spectroscopy*; Spiro, T. G., Ed.; John Wiley and Sons: New York, 1987; Vol. 2; p 59.
(33) Luecke, H.; Schobert, B.; Richter, H. T.; Cartailler, J. P.; Lanyi, J. K. *J. Mol. Biol.* **1999**, *291*, 899.
(34) Luecke, H.; Richter, H. T.; Lanyi, J. K. *Science* **1998**, *280*, 1934.
(35) Gai, F.; Hasson, K. C.; McDonald, J. C.; Anfinrud, P. A. *Science* **1998**, *279*, 1886.

(36) Hasson, K. C.; Gai, F.; Anfinrud, P. A. *Proc. Natl. Acad. Sci. U.S.A.* **1996**, *93*, 15124.
(37) Orlandi, G.; Zerbetto, F.; Zgierski, M. Z. *Chem. Rev.* **1991**, *91*, 867.
(38) Herbst, J.; Heyne, K.; Diller, R. *Science* **2002**, *297*, 822.
(39) Kobayashi, T.; Saito, T.; Ohtani, H. *Nature* **2001**, *414*, 531.
(40) Atkinson, G. H.; Blanchard, D.; Lemaire, H.; Brack, T. L.; Hayashi, H. *Biophys. J.* **1989**, *55*, 263.
(41) Blanchard, D.; Gilmore, D. A.; Brack, T. L.; Lemaire, H.; Hughes, D.; Atkinson, G. H. *Chem. Phys.* **1991**, *154*, 155.